

Article

Performances of the Synergy of Silica Fume and Waste Glass Powder in Ternary Blended Concrete

Moruf Olalekan Yusuf ^{1,*}, Khaled A. Alawi Al-Sodani ¹, Ali H. AlAteah ¹, Mohammed M. H. Al-Tholaia ¹, Adeshina A. Adewumi ¹, Azeez Oladipupo Bakare ², Abdullahi Kilaco Usman ¹ and Ibrahim Momohjimoh ³

¹ Department of Civil Engineering, College of Engineering, University of Hafr Al Batin, P.O. Box 1803, Hafr Al Batin 39524, Saudi Arabia; kalsodani@uhb.edu.sa (K.A.A.A.-S.); ali.alateah@uhb.edu.sa (A.H.A.); maltholaia@uhb.edu.sa (M.M.H.A.-T.); adeshina@uhb.edu.sa (A.A.A.); aukilaco@uhb.edu.sa (A.K.U.)

² Non-Destructive Evaluation Technology Department, University of Hafr Al Batin, P.O. Box 1803, Hafr Al Batin 39524, Saudi Arabia; abakare@uhb.edu.sa

³ Department of Mechanical Engineering Technology, Applied College, University of Hafr AlBatin, P.O. Box 1803, Hafr AlBatin 39524, Saudi Arabia; imomohjimoh@uhb.edu.sa

* Correspondence: moruf@uhb.edu.sa; Tel.: +966-552-545213

Abstract: The quest to enhance public health and the need for a reduction in the environmental solid wastes have prompted this study. Despite abundant studies on silica fume (SF or S) and waste glass powder (WGP or G), there is a need to understand the interaction of WGP with SF in the production of ordinary Portland cement (OPC or C)-based concrete using the water/binder ratio of 0.42. The investigated concrete comprised 90 wt.% of OPC and 10 wt.% of WGP+SF. The samples were denoted as C₉₀GxS_{10-x} such that x varied from 0–10 wt.% at the interval of 2.5. The findings revealed that an increase in the WGP/SF ratio enhanced the absorption of silica/glass blended concrete due to size incompatibility and proliferations of interfacial transition zones between the glass particle, silica fume and cement matrix. The density of fresh OPC concrete was higher than that of glass/silica blended concrete due to the difference in their relative densities. Incorporating WGP and SF in synergy enhanced silicate reorganization and led to a more amorphous binder and a reduction in hydroxyl-based compounds such as portlandite but caused microstructural heterogeneity in the morphology of the binder as obtained from XRD, FTIR and SEM/EDS results. The 28-day compressive strength of 46 MPa is achievable if the WGP and SF are kept within 2.5–5 wt.% and 5–7.5 wt.%, respectively. The study will foster the production of economic, environmental, and cost-efficient concrete.

Keywords: ternary blended concrete; glass waste powder; silica fume; strength; microstructure and absorption



Citation: Yusuf, M.O.; Al-Sodani, K.A.A.; AlAteah, A.H.; Al-Tholaia, M.M.H.; Adewumi, A.A.; Bakare, A.O.; Usman, A.K.; Momohjimoh, I. Performances of the Synergy of Silica Fume and Waste Glass Powder in Ternary Blended Concrete. *Appl. Sci.* **2022**, *12*, 6637. <https://doi.org/10.3390/app12136637>

Academic Editor: Lorena Zichella

Received: 12 June 2022

Accepted: 27 June 2022

Published: 30 June 2022

Publisher's Note: MDPI stays neutral with regard to jurisdictional claims in published maps and institutional affiliations.



Copyright: © 2022 by the authors. Licensee MDPI, Basel, Switzerland. This article is an open access article distributed under the terms and conditions of the Creative Commons Attribution (CC BY) license (<https://creativecommons.org/licenses/by/4.0/>).

1. Introduction

The world annual increase in cement production is to the tune of 2.5% with the gross production of about 4.6 billion tonnes. This has called for the exploration of alternative materials for the partial substitution and management of the proliferation of carbon dioxide into the atmosphere [1]. In several countries around the globe, the use of up to 60% supplementary cementitious materials for the sake of the economy and durability performance has been established. According to the Glass Packaging Institute (GPI), the recyclable glass content was about 3.1 million tons at an increase rate of 31.3%, while combusted glass was estimated to be 1.6 million tons. The glass in landfills was about 5.2% (7.6 million tons) of the total glass in municipal solid waste [2].

Previous studies have shown that the use of waste glass powder (WGP) as an active addition to concrete provides economic and environmental benefits [3], even if it is incorporated as a fine aggregate in white cement mortars [4]. Glass has been used as a supplementary cementitious material in several other studies [5–7], but in the majority of them it was recommended that 10–20 wt.% WGP can be utilized as a cement replacement

with a continuous decrease in compressive strength [8] reported that mortars with ground glass immersed in water for seven years have not shown signs of deterioration and have higher compressive strength. Even though glass has high alkali content, [9] asserted that it released only a very small fraction of sodium into the pore solution, thereby making it a safer additive.

Ibrahim et al. [10] reported the results of three concrete mixes comprising OPC, fly ash and silica fume. In all three mixes, the cement content was replaced by 0 wt.%, 5 wt.%, 10 wt.%, 15 wt.%, and 20 wt.% of waste glass powder. The results of the tests showed that WGP up to 5 wt.% can partially replace OPC in concrete that exhibits better tensile and compressive strengths than fly-ash- and silica-fume-based concrete. Additionally, a higher replacement of up to 20 wt.% WGP could reduce the tensile and compressive strengths by 13% to 14%, respectively. Despite the aforementioned, there are some disadvantages associated with utilizing glass in concrete such as a low early strength that could pose a challenge, especially where the early stripping of formwork is required in construction practice [11].

Silica fume, being a by-product of silicon and ferrosilicon alloy and environmental solid waste that contains about 75% silica [12], has the capability to contribute to the strength, as well as reduce the permeability and bleeding of concrete due to its pozzolanic effects [13]. It, however, has some setbacks, such as lowering the workability [14,15], and setting time of the concrete mixture [16] when the correct proportion is not used. The quantity of silica fume for an effective performance is reported to be in the range of 10–15 wt.% [17,18]. Waste glass powder (WGP), however, can contribute to the consistency of concrete mixture [19], due to its glassy surface with low water absorption. Both glass waste and silica fume up to 10–25 wt.% have been independently reported to contribute to compressive strength after a period exceeding 90 days [5]. Ref. [20] compared glass compositions with an observable increase in workability (flowability) and a decrease in setting time. A similar finding was reported by [21], while [22] reported a decrease in structural networks build up from 7.1 to 0.8 Pa/min with an increase in viscosity from 0.118 to 0.013 Pa/se. Another benefit of the use of glass waste was also derived from the use of cullet glass waste as a substitute for natural sand during the synthesis of an alkaline binder by using ground granulated blast furnace slag and fly ash as precursors. Positive results of durability performance were also reported for sand replacement by glass waste at the level of 25–100 wt.% within the temperature range of 200–800 °C [23,24].

Despite the benefits and setbacks that accompany the use of glass waste and silica fume independently, little information is available in the literature on how a combination of both materials can influence the synthesis of the binder with ordinary Portland cement in ternary blended concrete. This study aims at bridging this gap with a view to providing better understanding of their synergy in concrete production. The outcome from this study will provide an opportunity for more utilization of inorganic solid wastes in mortar and concrete production.

2. Materials and Methods

2.1. Materials

2.1.1. Glass Waste

Glass waste was collected from the dumpsite located along Sinaya, Hafr Al-Batin as shown in Figure 1. The glass was crushed first by a Los Angeles grinding machine before being further ground by an electronically controlled blending machine (titanium blade), which had a power rating of 1400 W operating on 220 V, 60 Hz. The glass powder was sieved through sieve No 200 or a 75-micron aperture. The oxide composition, as obtained from X-ray fluorescence, is presented in Table 1, while the X-ray diffractogram (XRD) is shown in Figure 2. The morphology of the particle is shown in Figure 3b. It reveals that glass powder is amorphous, as no phase could be identified except for a diffractive halo within a 2-theta angle, 20–30°.



Figure 1. Glass waste at dumpsite in Hafr Al-Batin.

Table 1. Oxide composition of raw materials.

| Oxides | Cement | Glass | Silica Fume |
|--|--------|-------|-------------|
| SiO ₂ | 20.17 | 68.1 | 95.85 |
| Al ₂ O ₃ | 5.58 | 0.9 | 0.26 |
| Fe ₂ O ₃ | 2.86 | 0.6 | 0.05 |
| CaO | 63.51 | 14.5 | 0.21 |
| MgO | 3.15 | 1.8 | 0.45 |
| Na ₂ O | 0.12 | 12.2 | - |
| K ₂ O | 0.57 | 0.8 | - |
| SO ₃ | 2.56 | 0.4 | 1.00 |
| SiO ₂ + Al ₂ O ₃ + Fe ₂ O ₃ | 26.89 | 69.6 | 96.16 |
| Specific gravity | 3.14 | 2.48 | |
| Specific surface area (m ² /kg) | 329.5 | 223.0 | >18,000 |
| LOI (wt.%) | 2.80 | 0.80 | 2.8 |

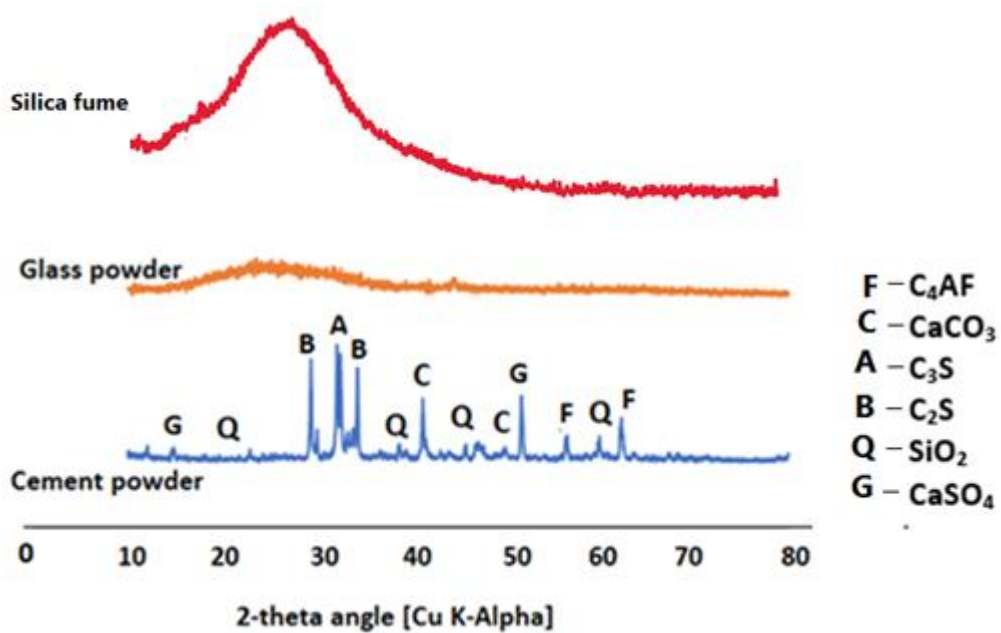


Figure 2. XRD diffractogram of the glass waste and cement powder.

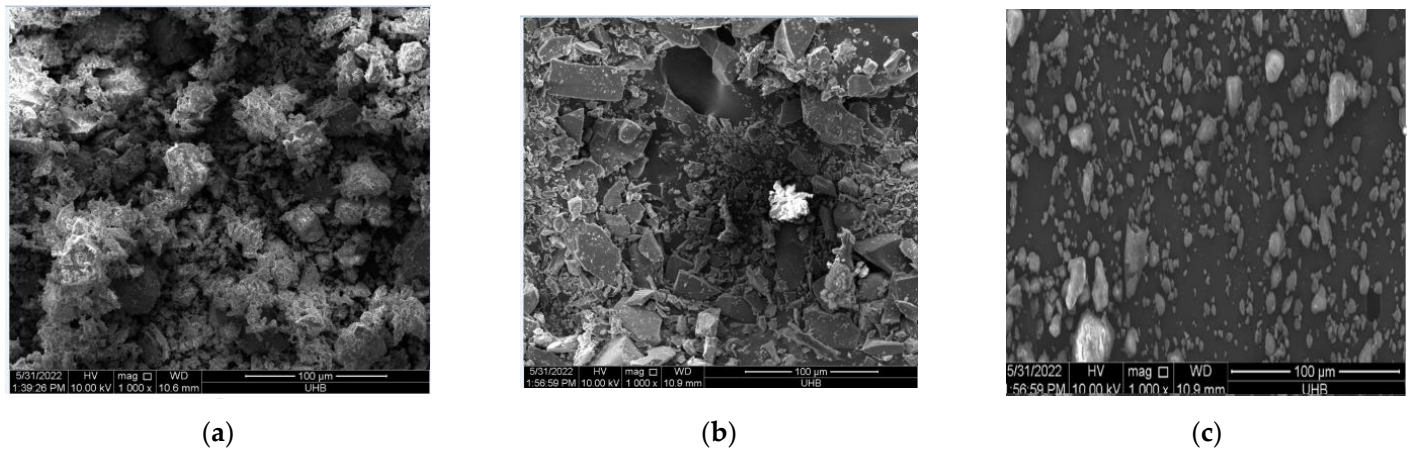


Figure 3. Morphology of (a) cement (b) glass waste (c) silica fume.

2.1.2. Ordinary Portland Cement

Type 1 cement was used in accordance with ASTM C 150 [25] with an apparent specific gravity in water of 3.15. The oxide composition is shown in Table 1, while Figure 2 shows the presence of alite (A), belite (B) and tetracalcium aluminoferrite (F) among other phases present in cement. Figure 3a indicates the morphology of cement particle.

The specific surface areas (BET) of cement, WGP and silica fume were determined using Micromeritics ASAP2020 via nitrogen gas adsorption. The morphology of WGP and cement powder were evaluated using a JSM-5800LV scanning electron microscope (Figure 3).

2.1.3. Silica Fume

Table 1 shows the oxide composition of the silica fume (SF) that was used in this study with $\text{SiO}_2 + \text{Al}_2\text{O}_3 + \text{Fe}_2\text{O}_3$ amounting to 96.2 % as shown in Table 1, while the XRD is shown in Figure 2. The morphologies of the raw materials are shown in Figure 3a–c. The specific gravity of the SF was 2.25 and it was used in concrete in accordance with [26].

2.1.4. Superplasticizer

Commercially available Glenum[®] superplasticizer of 0.5 wt% of binder was used to enhance the workability of the concrete.

2.1.5. Fine Aggregates

Natural sand of specific gravity of 2.71 that passed a sieve of 2.36 mm (No. 8) corresponding to [27] was used in the concrete production.

2.1.6. Coarse Aggregate

Coarse limestone aggregates with sizes ranging from 8 mm to 14 mm and a specific gravity of 2.54 were used. They were used in the mix in a saturated surface dry (SSD) condition and the proportion was as shown in Table 2.

Table 2. Distribution of coarse aggregates.

| Coarse Aggregate Size (mm) | Percentage Composition |
|----------------------------|------------------------|
| 8 | 30 |
| 10 | 20 |
| 12 | 30 |
| 14 | 20 |

2.2. Experimental Tests

2.2.1. Workability

The workability of the concrete was tested using the slump cone test in accordance with [28].

2.2.2. Setting Time

The initial and final setting times of the blended cement/glass paste were determined in accordance with [29].

2.2.3. Water Absorption

Water absorption was determined by submerging the samples of dimensions of 100 mm × 100 mm × 100 mm into water until saturation. A textile fabric towel was then used to dry the sample surface to achieve the saturated dry surface whose mass was recorded as M_{ssd} . The samples were then put in the oven at the temperature of 105 °C for 24 h to determine the dry mass (M_{oven}) in accordance with [30]. The water absorption was then calculated as shown in Equation (1):

$$\text{Water absorption} = \frac{M_{ssd} - M_{oven}}{M_{oven}} \times 100 \quad (1)$$

2.2.4. Compressive Strength

The compressive strength of the concrete was determined by using cubic samples of dimensions 100 mm × 100 mm × 100 mm. The compressive strength test was determined by using universal testing machine at the loading rate of 0.9 kN/s. The average of triplicate samples was recorded at 3, 7, 14 and 28 days.

2.3. Characterization and Morphology of the Specimens

To determine the bond behaviour, morphology/elemental composition and the nature of the formed compound, Fourier transform spectroscopy (FTIR), scanning electron microscopy/energy dispersive X-ray spectroscopy (SEM + EDS) and the X-ray diffractometer (XRD) were used, respectively. An XRD Bruker instrument model d2-Phaser with Cu Ka radiation (40 kV, 40 mA) was used to determine the phases of the mineral compounds by continuous scanning within the angle 2-theta range of 4–80° and at a scan speed of 2.5°/min. FTIR was determined using a Perking Elmer 880 spectrometer while the microstructural characterization of the paste sample was conducted with a JEOL SEM + EDS model 5800 LV at the accelerating voltage of 20 kV.

2.4. Sample Preparation

2.4.1. Sample Designation

The quantities of cement glass and silica fume in the proportion were prepared such that cement content was 90 wt.% while WGP+SF was 10 wt.% for the production of the ternary blended binder [31]. The samples were denoted with the acronym $C_{90}G_xS_{10-x}$ such that x varied from 0–10% at the interval of 2.5 while $C_{100}G_0S_0$ (cement only) concrete served as the control.

2.4.2. Mix Design

The concrete samples were made based on the mixed design shown in Table 3. The water–cement ratio was maintained at 0.42 and the total mass of the binders in 1 m³ of concrete content was 350 kg. The total silica fume and glass powder was maintained at the constant percentage of 10% with glass-powder-to-silica-fume ratios of 0:10%, 2.5:7.5%, 5:5%, 7.5:2.5% and 10:0% while ordinary Portland cement was maintained at 90% of the binder in the concrete.

Table 3. Mix design for glass-blended silica-fume concrete.

| Mixes | Percentage Glass | Cement (kg/m ³) | Glass (kg/m ³) | SF (kg/m ³) | Initial Water (kg/m ³) | SP (kg/m ³) | Fine Agg (kg/m ³) | Coarse Agg (kg/m ³) |
|---|------------------|-----------------------------|----------------------------|-------------------------|------------------------------------|-------------------------|-------------------------------|---------------------------------|
| C ₁₀₀ G ₀ S ₀ | 0.0% | 350 | 0 | 0 | 147 | 1.75 | 798 | 1093 |
| C ₉₀ G ₀ S ₁₀ | 0.0% | 315 | 0 | 35 | 147 | 1.75 | 786 | 1093 |
| C ₉₀ G _{2.5} S _{7.5} | 2.5% | 315 | 8.75 | 26.25 | 147 | 1.75 | 787 | 1093 |
| C ₉₀ G ₅ S ₅ | 5.0% | 315 | 17.5 | 17.5 | 147 | 1.75 | 788 | 1093 |
| C ₉₀ G _{7.5} S _{2.5} | 7.5% | 315 | 26.25 | 8.75 | 147 | 1.75 | 789 | 1093 |
| C ₉₀ G ₁₀ S ₀ | 10.0% | 315 | 35 | 0 | 147 | 1.75 | 790 | 1093 |

2.4.3. Concrete Mixing Procedure

The required quantities of materials were proportioned in accordance with Table 3. Mixing was performed with the aids of a rotary mixer in three stages and in accordance with ASTM C 192 [32]. First, cement, glass and silica fume were added together and mixed dry for 3 min, while superplasticizer was added to water before being added to the dry powders and then mixed for another 3 min. Fine aggregates and coarse aggregates were separately added for 2 min each. The mixer and its contents were kept in oscillation for an additional 2 min, mixing at high speed to achieve a homogenous mixture. The resulting concrete was placed in the oil-smearred 100 mm × 100 mm × 100 mm mould in three layers, and then compacted for 30 s each by using table vibrator. Compaction is necessary to remove any entrapped air. This was then followed with scrapping and levelling of the concrete to the surface of the moulds. The concrete samples were then covered with a plastic sheet to prevent moisture loss. Afterwards, the specimens were kept in the laboratory at 20 ± 5 °C and then demoulded after 24 hrs before placing them in the curing tank. Compressive tests were conducted at 3, 7, 14 and 28 days.

3. Discussion of Results

3.1. Effect of Glass and Silica Fume Synergy on the Concrete Workability

It is apparent that the presence of silica fume (10 wt.%) significantly reduces the workability of the concrete due to its fineness, as shown in Figure 4. This is not different from what has been previously reported in the literature (Banja and Sengupta, 2004). It is worthy to note that the presence of waste glass powder (WGP) in synergy with silica fume at 1:3 and 1:1 denoted as C₉₀G_{2.5}S_{7.5} and C₉₀G₅S₅, respectively, reduced the consistency in comparison with C₁₀₀G₀S₀ by 55.6% and 11.11%, respectively. This suggests that the combination of silica fume (SF) and GWP waste influences the workability of the mixture. The impact of the spherical shape of SF (Figure 3c) in the presence of WGP contributed to the concrete flow as noticed in C₉₀G_{2.5}S_{7.5} (75 mm slump), compared to the sample in which it was absent (C₉₀G_{2.5}S₀), for which the slump value was 55 mm. The reduction in the consistency of SF-free concrete in the presence of WGP was due to the angularity of its shape (Figure 3b), thereby generating more interparticle frictional resistance. Despite such an effect, the consistency of GWP-based concrete was still higher than that of the ordinary Portland cement (OPC) concrete [21] for which the slump was 45 mm. The resultant effect of SF and GWP in the ternary blended concrete can therefore be said to contribute to its consistency and cohesiveness.

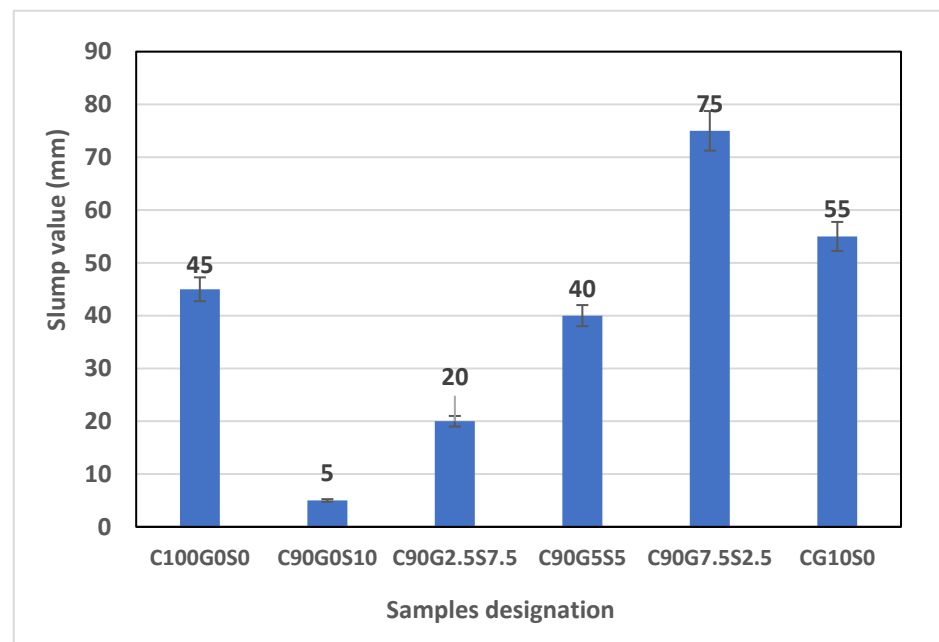


Figure 4. Effect of silica fume/waste glass powder synergy on concrete workability.

3.2. Effect of Silica Fume/Glass Powder Interaction on the Absorption of the Concrete

Figure 5 shows that the presence of waste glass powder (WGP) in blended silica-fume (SF) concrete enhances the absorption of the concrete due to the presence of interfacial transition zones (ITZs) between the irregularly shaped glass and the cement matrix. Even though it is well known that SF reduces the absorption of blended concrete by the micro-filling effect, the effect of microcracks within the region of the ITZ (SEM morphology, Figure 6), due to higher porosity, preponderates that in $C_{90}G_xS_{10-x}$ (ternary blended concrete). This is well noticed in the sample where WGP outweighed SF or where SF was completely absent, such as in $C_{90}G_{7.5}S_{2.5}$ and $C_{90}G_{10}S_0$. The lowest absorption (1.68%) was recorded in the blended SF concrete $C_{90}G_0S_{10}$ and the worst performance was recorded in $C_{90}G_{10}S_0$ (6.15%), while those of $C_{90}G_{7.5}S_{2.5}$ and $C_{90}G_5S_5$ were comparable within 3.44–3.55%, as shown in Figure 5.

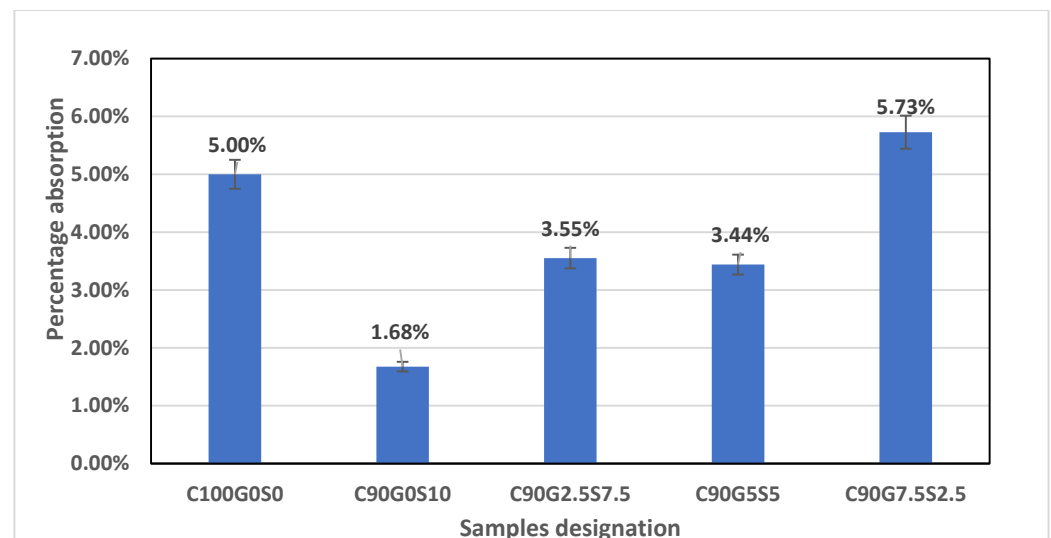


Figure 5. Water absorption in blended silica-fume/glass concrete.

3.3. Effect of Silica Fume and Glass Powder Combination on the Fresh Density of the Concrete

The specific gravity of SF and WGP were lower than that of the OPC, therefore the combination of glass and silica fume generated a lighter concrete compared to the OPC concrete. Besides, the higher the proportion of the glass in the mixture, the denser the fresh density of the ternary blended concrete ($C_{90}G_xS_{10-x}$), but lower than the density of the OPC ($C_{100}G_0S_0$) concrete. The highest density was observed in $C_{90}G_0S_0$ and then followed by $C_{90}G_{10}S_0$, while the least was in $C_{90}G_0S_{10}$. The fresh density of the OPC concrete was 2390 kg/m^3 , as shown in Figure 7, and then reduced by 1%, 1.8%, 1.5%, 0.4% and 0.1% as the glass-to-silica-fume proportion increased from 0 to 10 wt%. and as SF reduced from 10 to 0 wt.%, at an interval of 2.5 wt.%, respectively.

From Figure 8, the inclusion of WGP and SF in ternary blended concrete reduced the early strength development due to the dilution effect of the nucleation site. This can be observed in the 3- and 7-day strength in $C_{90}G_0S_{10}$ and $C_{90}G_{10}S_0$ with a reduction of 8.4% and 18.8%, respectively. There was a further reduction to 17% upon the inclusion of 7.5% WGP in synergy with 2.5% silica fume ($C_{90}G_{2.5}S_{7.5}$). However, the interaction of glass and silica fume reduced the dilution effect, as can be seen in $C_{90}G_5S_5$. This implies that the presence of silica fume and glass powder in concrete could reduce the dilution effect, which could affect the early strength in blended concrete. The presence of glass powder reduced the rate of the pozzolanic reaction, thereby reducing the later strength development, as noticed at 28 days. The rate of strength development was significant over 28 days in glass-free, blended silica-fume concrete ($C_{90}G_0S_{10}$) in comparison with the blended samples ($C_{90}G_{2.5}S_{7.5}$, $C_{90}G_5S_5$, $C_{90}G_{7.5}S_{2.5}$, $C_{90}G_{10}S_0$). Additionally, comparing $C_{90}G_{7.5}S_{2.5}$ with $C_{90}G_{2.5}S_{7.5}$ implies that SiO_2 in silica fume could be said to be more reactive compared to the available glass powder. Figure 2 corroborates this fact as the diffractive halo in the silica fume X-ray diffractogram is more pronounced than that of WGP.

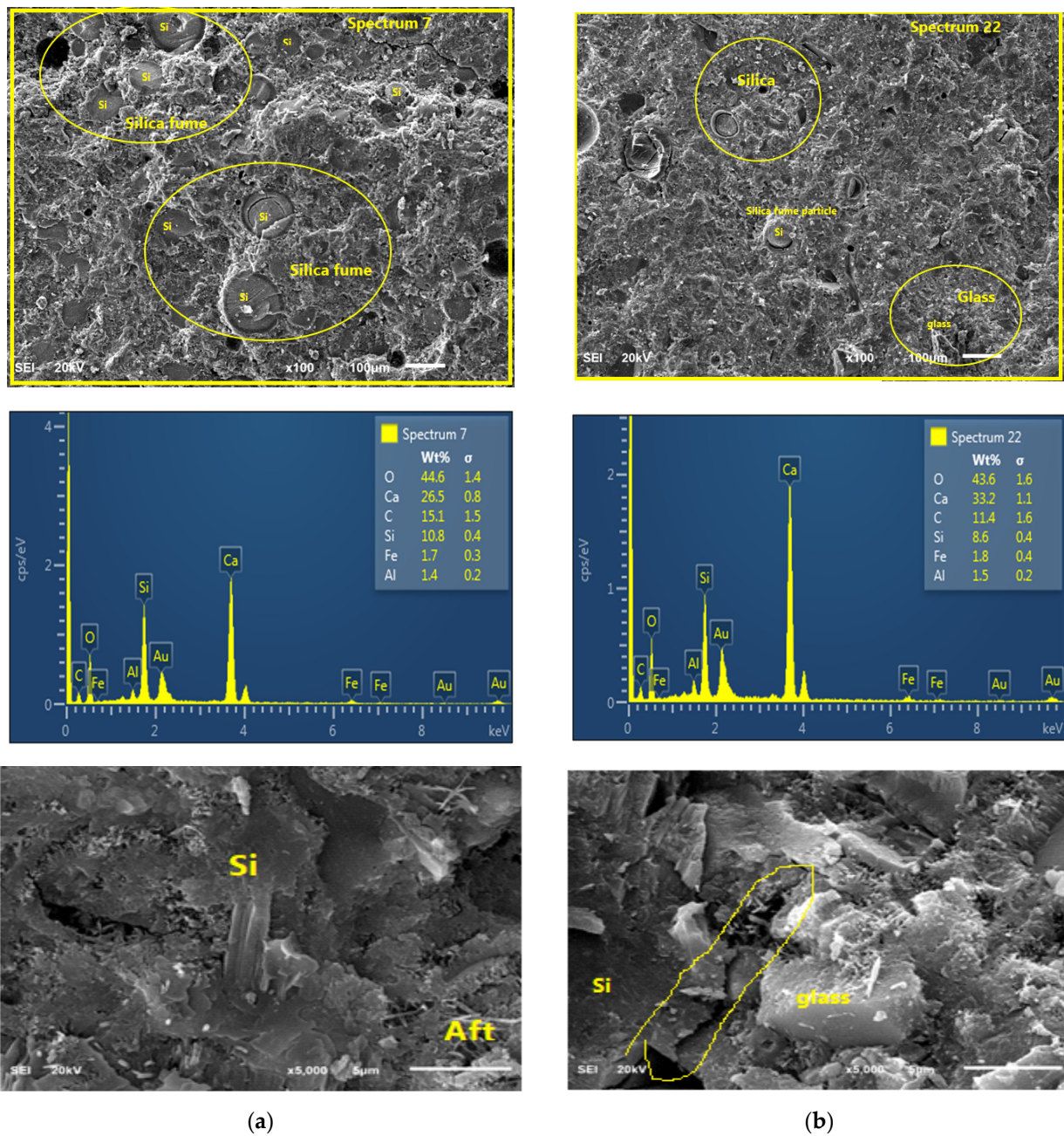


Figure 6. Morphology of silica fume (binary) blended paste (left) in comparison with the silica fume/glass (ternary) paste (right). (a) Silica-fume blended paste. (b) Silica-fume/glass-powder (ternary) paste.

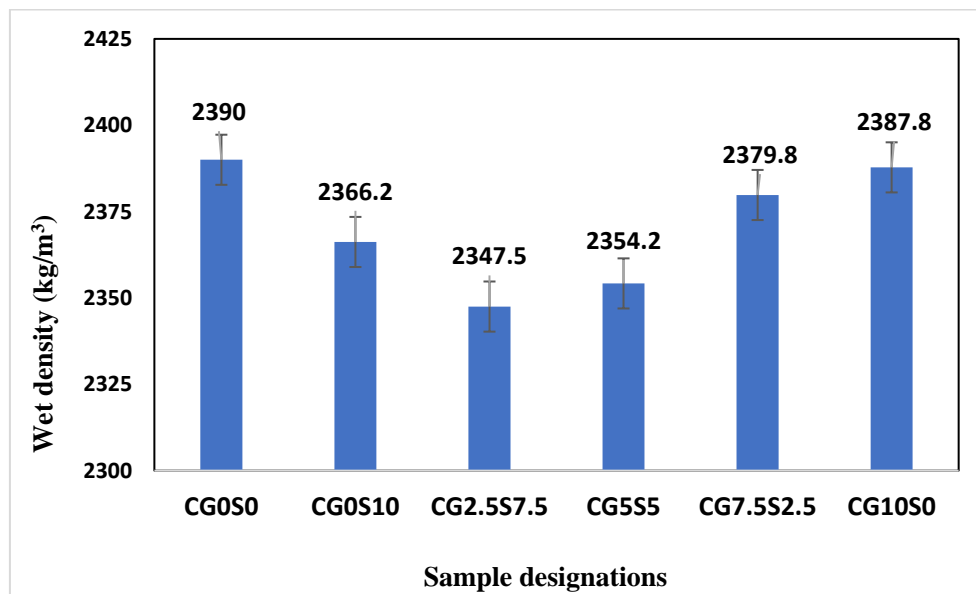


Figure 7. Density of the fresh blended silica-fume/glass concrete.

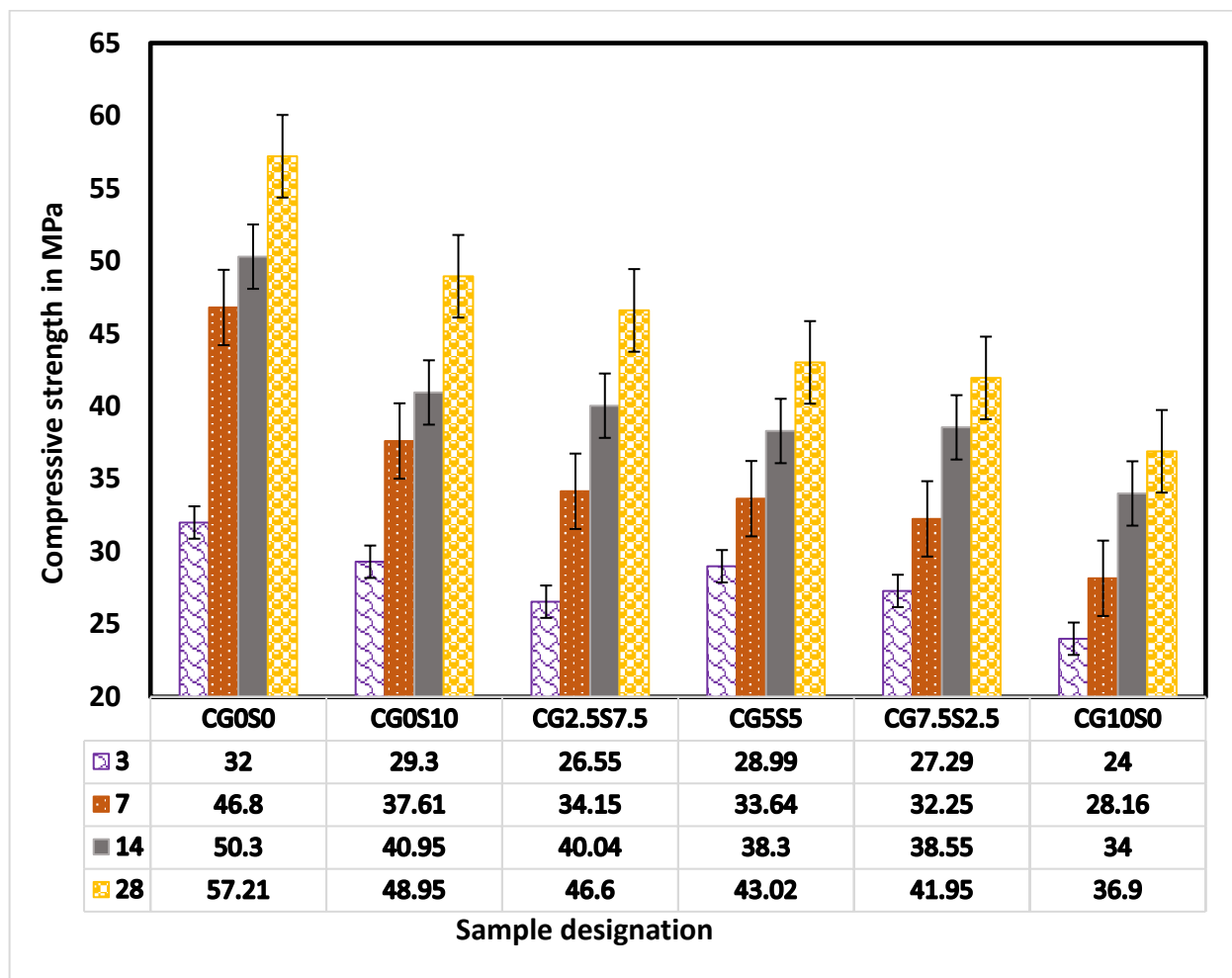


Figure 8. Concrete compressive strength and synergistic effect of silica fume and glass powder.

3.4. Fourier Transform Spectroscopy Details on Compressive Strength

From Figure 9, the combination of glass powder and silica fume affects the bond characteristics of the binder. The silicate organization in the OPC binder is different from the blended glass/silica-fume concrete. The Si-O-Si vibration at 966 cm^{-1} is grossly affected due to the infusion of additional amorphous silica from two different sources. This causes the broadening of this band, which suggests more silicate concatenation in blended, glass-infused silica-fume concrete. The vibration of sulphate bonds in gypsum is equally affected at the wavenumbers of 1115 , 1107 and 1130 cm^{-1} for the OPC, blended silica-fume and ternary (glass and SF) blended binders, respectively. The presence of amorphous silica in glass or SF could cause changes in the chemical composition of the binder either by infusing Si in portlandite to form CSH or in the hydration of C_3A or C_4AF compounds to form hydrogarnet (CASH). The changes in the configuration of portlandite also caused the decrease in the carbonation of the ternary binder. The vibration of the $\text{O}=\text{C}=\text{O}$ bond was more pronounced with a stronger peak at 1437 cm^{-1} , but appears to broaden and flatten out in the presence of amorphous silica in both WGP and SF. This suggests that amorphous silica in supplementary cementitious materials could cause a reduction in the carbonation process by pore blockage in the aftermath of secondary hydration. Similarly, the vibration of the $\text{O}=\text{C}=\text{O}$ bonds from CO_2 from CO_3^{2-} (calcite) at the wavenumber of 2347 cm^{-1} was sparingly observed in the blended silica/glass (ternary) binder. The reduction in hydroxyl-based compounds in glass/silica-fume concrete caused the OH^- vibration peak at 3642 cm^{-1} to become shallow with the reduced intensity and vibrational frequency at the wavenumbers of 3638 cm^{-1} and 3433 cm^{-1} in the binary silica-fume ($\text{C}_{90}\text{G}_0\text{S}_{10}$) and ternary blended silica/glass ($\text{C}_{90}\text{G}_x\text{S}_{10-x}$) concretes, respectively. In this regard, the incorporation of WGP and SF in blended concrete further enhanced its durability in terms of the reduction in carbonation due to the consumption of portlandite to form CSH.

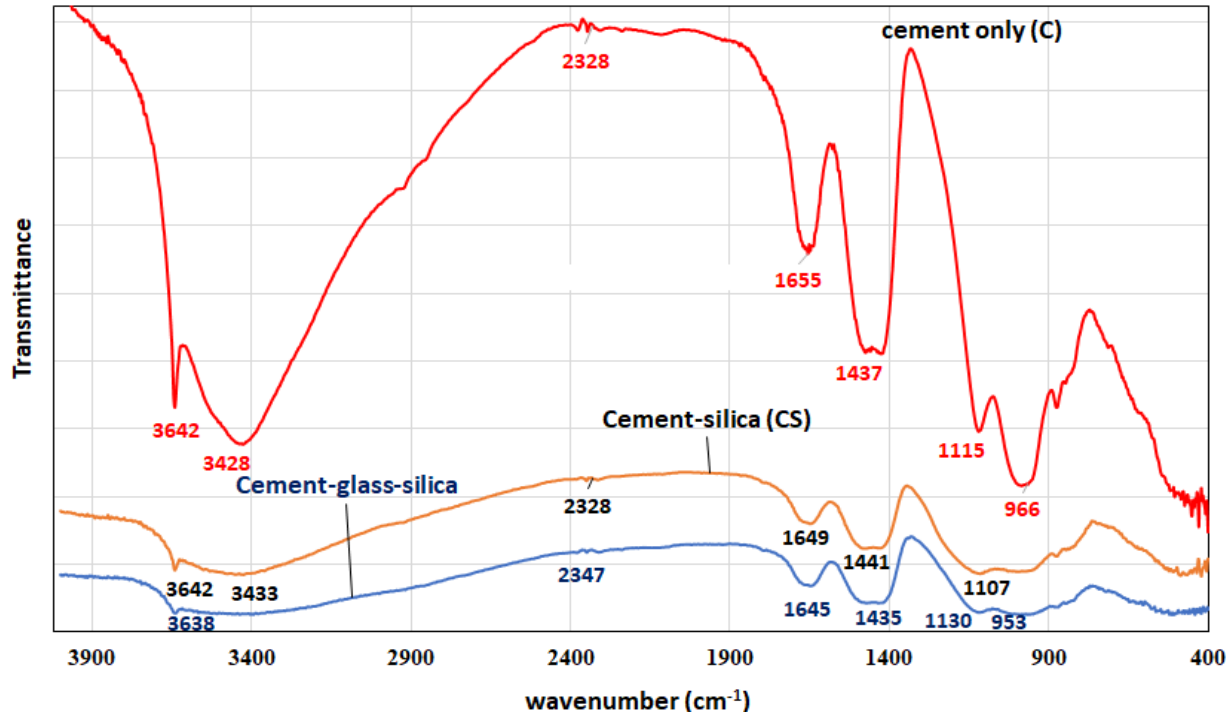


Figure 9. FTIR spectra of blended silica-fume/glass (ternary) cement (CGS—bottom), blended silica-fume (binary) cement (CS—middle) and hydrated cement (CC—top) paste.

3.5. Effect of Elemental Ratio on the Concrete Characteristics

Generally, the spectrum of blended silica-fume paste indicates that the Ca/Si ratio decreased with the increase in the amount of amorphous silica present in the products, as

shown in Table 4 by the energy dispersion spectroscopy (EDS) results. Region 8 (Figure 10) comprises both calcium silica hydrate (CSH) and calcium aluminosilicate hydrate (CASH).

Table 4. Elemental ratio in silica fume and glass-blended silica-fume paste.

| Elements | Silica-Cement | Glass-Silica-Cement |
|----------|---------------|---------------------|
| Ca/Si | 3.34 | 3.78 |
| Si/Al | 7.11 | 4.20 |
| Ca/C | 2.75 | 3.98 |
| Ca/F | 2.04 | 19.74 |

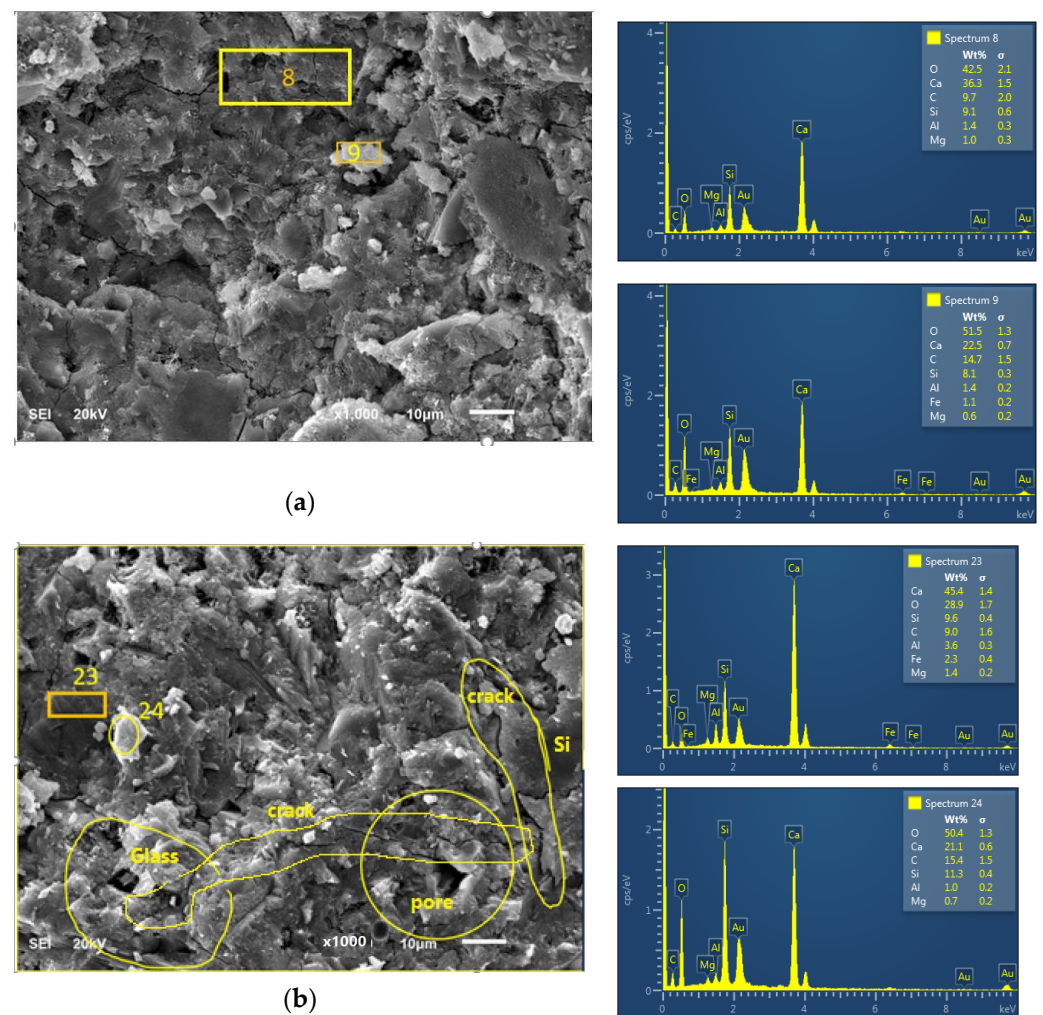
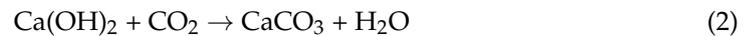


Figure 10. X-ray diffraction spectroscopy of the silica fume and glass/silica-fume binder. (a) Silica-fume blended paste (b) Glass/silica-fume ternary blended paste.

The interaction of amorphous silica with tetracalcium aluminosilicate (C_4AF) and tricalcium silicate (C_3A) led to the formation CASH, as indicated in region 8 of the blended silica-fume paste. Spectra 9 and 23 have the presence of Fe but spectra 8 and 24 do not. The Ca/Fe ratio was 19.73 in the ternary blended paste, but drastically reduced to 2.04 in the absence of glass powder. This suggests that glass induces the reactivity of C_4AF hydrations that could lead to the formation of hydrogarnet (CASH). Moreover, a lower calcium–carbon ratio ($Ca/C = 2.75$) in the blended silica binder in contrast to 3.78 in the blended glass/silica-fume (ternary) samples indicates that glass changes the nucleation site

of the hydration products within the matrix through the infusion of amorphous silica into portlandite to form CSH by preventing or limiting the occurrence of Equation (2).



This explains why carbonation was noted to have reduced by the incorporation of glass in the blended silica-fume- or OPC-based concrete. Similarly, the microstructure shown in Figure 10 in the glass/silica binder was found to be non-uniform and full of micropores due to the heterogeneity or incompatibility of the glass particle with both the cement and silica-fume particle sizes thereby causing more ITZs within the crack region (Figure 10b).

Figure 11 shows the diffractogram of ternary (glass/silica fume) blended paste (SGC), blended silica-fume (SC) paste and hydrated cement paste (CMT). The SGC paste was more amorphous compared to the SC and CMT. The inclusion of glass induced the formation of larnite (L-hydrated calcium silicate compound, 2CaOSiO_2 PDF#96-200-0096) around the 2-theta angle of 39.5° (Region 2) while calcite (CaCO_3 -CC-PDF#99-200-0080) formation was noticed to reduce in the SGC compared to SC. This was due to the additional pozzolanic effects that caused the conversion of portlandite (P- PDF# 96-900-8367) to additional CSH via a secondary hydration, as shown in Equations (2) and (3) (Figure 11).

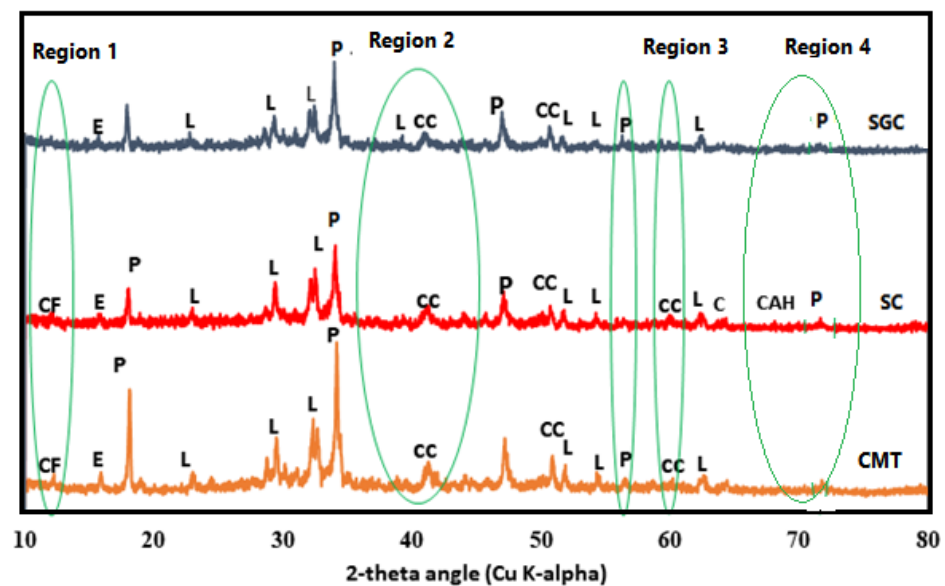


Figure 11. X-ray diffractogram of glass-blended silica-fume concrete.

The presence of amorphous silica interferes with tricalcium aluminate (C_3A) in the process of the formation of early ettringite and the hydration of C_4AF (CF PDF#96-200-0015) to form calcium aluminosilicate silicate hydrate (CA(S)H —Region 2, Figure 11) or an octahedral form of hydrogarnet [33–35]. The absence of the peak of C_4AF (CF PDF#96-200-0015—Region 1) suggested the possibility of such a reaction. The ettringite formed in glass-infused silica-fume concrete was seen to be less ordered in comparison with the OPC concrete (Figure 11).

The reaction of gypsum with C_3A and CF increased the setting time due to the formation of ettringite $\text{C}_3\text{A} \cdot 3\text{CaSO}_4 \cdot 32\text{H}_2\text{O}$ ($\text{E-AlCa}_3\text{H}_{34}\text{O}_{24.5}\text{S}_{1.5}$ —PDF# 99-200-0093) at 2-theta angle of $10\text{--}13^\circ$ or led to the later formation of monosulphate hydrate ($\text{C}_3\text{A} \cdot \text{CaSO}_4 \cdot 12\text{H}_2\text{O}$) in the excess of belite (C_2S). It has been reported [33,34] that amorphous silica could modify the hydration of CF and C_3A to form hydrogarnet (CAH —Region 4). The formation of hydrogarnet [$3\text{CaO}(\text{Al} \cdot \text{Fe})_2\text{O}_3 \cdot 3(\text{H}_2\text{O}) \cdot 2\text{SiO}_2$] is supported by the presence of Ca, Al and Fe in the EDS in spectra 9 and 23 (Figure 10).

4. Conclusions

The use of environmental waste in concrete production is very important to improving the characteristics and cost efficiency of the resultant concrete on one hand, and to get rid of the solid waste culminating against public health on the other. This study has investigated the impact of the ternary blending of ordinary Portland cement (OPC), waste glass powder (WGP) and silica-fume (SF) powders on the fresh property, workability, strength, bond characteristics and microstructure of the concrete. The conclusions are the following:

- Glass addition to silica-fume concrete synergistically enhances the workability of the concrete
- The blending of glass powder with silica fume in OPC concrete increased its water absorption due to the proliferation of interfacial transition zones, which arose from the size incompatibility between the silica fume, glass particle and OPC particles. Silica fume reduced the absorption of concrete owing to the microfilling effect, while WGP enhanced it due to shape angularity and its higher capillary action that enhances water molecule transfer to adjacent particles.
- The fresh or wet density of OPC concrete ($C_{100}G_0S_0$) was found to be more than that of ternary blended (WGP, SF and OPC) concrete due to the higher relative density of cement (3.15) in comparison with WGP and SF.
- Fourier transform infrared (FTIR) spectroscopy and X-ray diffraction (XRD) revealed that the incorporation of WGP in synergy with blended SF concrete enhanced silicate reorganization, enhanced the product amorphousness and reduced hydroxyl-based compounds such as portlandite due to amorphous silica infusion.
- The addition of glass waste in blended silica-fume concrete caused heterogeneity in the microstructure and the proliferation of weak interfacial transition zones, leading to the formation of microcracks in the morphology as noted in the scanning electronic microscope and energy dispersive spectroscopy (SEM/EDS) results.
- Economic and cost-efficient ternary blended concrete with a 28-day compressive strength beyond 40 MPa can be produced if the WGP is partly and synergistically substituted for SF such that the percentages of glass waste and silica fume are kept within 2.5–5% and 5–7.5%, respectively.

Author Contributions: Conceptualization, M.O.Y.; Formal analysis, M.O.Y. and A.O.B.; Funding acquisition, M.O.Y.; Investigation, M.M.H.A.-T. and A.K.U.; Methodology, M.O.Y., A.A.A. and I.M.; Project administration, A.A.A.; Supervision, M.O.Y. and A.H.A.; Writing—original draft, M.O.Y.; Writing—review & editing, K.A.A.A.-S. All authors have read and agreed to the published version of the manuscript.

Funding: The authors extend their appreciation to the Deanship for Research & Innovation, Ministry of Education in Saudi Arabia for funding this research work through the project No: IFP-A-2022-2-1-10.

Institutional Review Board Statement: Not applicable.

Informed Consent Statement: All authors consent to the publication.

Acknowledgments: The authors would like to appreciate the remarks of the anonymous reviewers which have greatly improved the manuscript. The continuous support of University of Hafr Al Batin is appreciated.

Conflicts of Interest: The authors declare no conflict of interest.

References

1. Mehta, A.; Kar, D.; Ashish, K. Silica fume and waste glass in cement concrete production: A review. *J. Build. Eng.* **2020**, *29*, 100888. [[CrossRef](#)]
2. United State Environmental Protection Agency (EPA). Facts and Figures about Materials, Waste and Re-cycling, Glass: Material-Specific Data. 2021. Available online: <https://www.epa.gov/facts-and-figures-about-materials-waste-and-recycling/glass-material-specific-data> (accessed on 12 June 2022).

3. Maraghechi, H.; Maraghechi, M.; Rajabipour, F.; Pantano, C.G. Pozzolanic reactivity of recycled glass powder at elevated temperatures: Reaction stoichiometry, reaction products and effect of alkali activation. *Cem. Concr. Compos.* **2014**, *53*, 105–114. [[CrossRef](#)]
4. Ling, T.-C.; Poon, C.-S.; Kou, S.-C. Feasibility of using recycled glass in architectural cement mortars. *Cem. Concr. Compos.* **2011**, *33*, 848–854. [[CrossRef](#)]
5. Islam, G.S.; Rahman, M.; Kazi, N. Waste glass powder as partial replacement of cement for sustainable concrete practice. *Int. J. Sustain. Built Environ.* **2017**, *6*, 37–44. [[CrossRef](#)]
6. He, Z.-H.; Zhan, P.-M.; Du, S.-G.; Liu, B.-J.; Yuan, W.-B. Creep behavior of concrete containing glass powder. *Compos. Part B Eng.* **2019**, *166*, 13–20. [[CrossRef](#)]
7. Patel, D.; Tiwari, R.P.; Shrivastavad, R.; Yadav, R.K. Effective utilization of waste glass powder as the substitution of cement in making paste and mortar. *Constr. Build. Mater.* **2019**, *199*, 406–415. [[CrossRef](#)]
8. Carsana, M.; Frassoni, M.; Bertolini, L. Comparison of ground waste glass with other supplementary cementitious materials. *Cem. Concr. Compos.* **2014**, *45*, 39–45. [[CrossRef](#)]
9. Schwarz, N.; Neithalath, N. Influence of a fine glass powder on cement hydration: Comparison to fly ash and modeling the degree of hydration. *Cem. Concr. Res.* **2008**, *38*, 429–436. [[CrossRef](#)]
10. Ibrahim, K.I.M. Recycled waste glass powder as a partial replacement of cement in concrete containing silica fume and fly ash. *Case Stud. Constr. Mater.* **2021**, *15*, e00630. [[CrossRef](#)]
11. *ASTM C192*; Standard Practice for Making and Curing Concrete Test Specimens in the Laboratory. ASTM International: West Conshohocken, PA, USA, 2018.
12. Toutanji, H.; Delatte, N.; Aggoun, S.; Duval, R.; Danson, A. Effect of supplementary cementitious materials on the compressive strength and durability of short-term cured concrete. *Cement Concr. Res.* **2004**, *34*, 311–319. [[CrossRef](#)]
13. Bagheri, A.; Zanganeh, H.; Moalemi, M.M. Mechanical and durability properties of ternary concretes containing silica fume and low reactivity blast furnace slag. *Cem. Concr. Compos.* **2012**, *34*, 663–670. [[CrossRef](#)]
14. Hasan-Nattaj, F.; Nematzadeh, M. The effect of forta-ferro and steel fibers on mechanical properties of high-strength concrete with and without silica fume and nano-silica. *Constr. Build. Mater.* **2017**, *137*, 557–572. [[CrossRef](#)]
15. Fallah, S.; Nematzadeh, M. Mechanical properties and durability of high-strength concrete containing macro-polymeric and polypropylene fibers with nano-silica and silica fume. *Constr. Build. Mater.* **2017**, *132*, 170–187. [[CrossRef](#)]
16. Justice, J.M.; Kennison, L.H.; Mohr, B.J.; Beckwith, S.L.; McCormick, L.E.; Wiggins, B.; Zhang, Z.Z.; Kurtis, K.E. Comparison of Two Metakaolins and a Silica Fume Used as Supplementary Cementitious Materials. In *Seventh International Symposium on Utilization of High Strength/High Performance Concrete*; American Concrete Institute: Indianapolis, IN, USA, 2005; pp. 1–88.
17. Mazloom, A.A.M.; Ramezani-pour, J.J.B. Effect of silica fume on mechanical properties. *Cement Concr. Compos.* **2004**, *26*, 347–357. [[CrossRef](#)]
18. Khayat, K.H.; Aitcin, P.C. Silica Fume: A Unique Supplementary Cementitious Material. In *Mineral Admixtures in Cement and Concrete*; Ghosh, S.N., Ed.; ABI Books Private Limited: New Delhi, India, 1993; pp. 227–265.
19. Aliabdo, A.A.; Abd Elmoaty, A.E.M.; Aboshama, A.Y. Utilization of waste glass powder in the production of cement and concrete. *Constr. Build. Mater.* **2016**, *124*, 866–877. [[CrossRef](#)]
20. Lu, J.-X.; Duan, Z.; Poon, C.S. Fresh properties of cement pastes or mortars incorporating waste glass powder and cullet. *Constr. Build. Mater.* **2017**, *131*, 793–799. [[CrossRef](#)]
21. Rahma, A.; El Naber, N.; Ismail, S.I. Effect of glass powder on the compression strength and the workability of concrete. *Cogent Eng.* **2017**, *4*, 7. [[CrossRef](#)]
22. Sadati, S.; Khayat, K.H. Rheological and hardened properties of mortar incorporating high-volume ground glass fiber. *Constr. Build. Mater.* **2017**, *152*, 978–989. [[CrossRef](#)]
23. Sasui, S.; Kim, G.; Nam, J.; van Riessen, A.; Hadzima-Nyarko, M. Effects of waste glass as a sand replacement on the strength and durability of fly ash/GGBS based alkali activated mortar. *Ceram. Int.* **2021**, *47*, 21175–21196. [[CrossRef](#)]
24. Khan, M.N.N.; Sarker, P.K. Effect of waste glass fine aggregate on the strength, durability and high temperature resistance of alkali-activated fly ash and GGBFS blended mortar. *Constr. Build. Mater.* **2020**, *263*, 120579. [[CrossRef](#)]
25. *ASTM C150-07*; Standard Specification for Portland Cement. ASTM International: West Conshohocken, PA, USA, 2017.
26. *ASTM C1240-20*; Standard Specification for Silica Fume Used in Cementitious Mixtures. ASTM International: West Conshohocken, PA, USA, 2020.
27. *ASTM C 157*; Standard Test Method for Length Change of Hardened Hydraulic-Cement Mortar and Current. ASTM International: West Conshohocken, PA, USA, 2010; pp. 1–7. [[CrossRef](#)]
28. *ASTM C 143*; Significance of Tests and Properties of Concrete and Concrete Aggregate. ASTM International: West Conshohocken, PA, USA, 1956. Available online: https://books.google.co.uk/books?id=plRnBOM30TEC&pg=PA38&redir_esc=y#v=onepage&q&f=false (accessed on 12 June 2022).
29. *ASTM C191-21*; Standard Test Methods for Time of Setting of Hydraulic Cement by Vicat Needle. ASTM International: West Conshohocken, PA, USA, 2021.
30. *ASTM C642*; Standard Test Method for Density, Absorption, and Voids in Hardened Concrete. ASTM International: West Conshohocken, PA, USA, 2021.

31. ASTM C 595; Standard Specification for Blended Hydraulic Cements. 98(Reapproved); ASTM International: West Conshohocken, PA, USA, 2000; pp. 1–5. [[CrossRef](#)]
32. ASTM C192/C192M; Standard Practice for Making and Curing Concrete Test Specimens in the Laboratory. ASTM International: West Conshohocken, PA, USA, 2016; pp. 1–8.
33. Siauciunas, R.; Baltusnikas, A. Influence of SiO₂ Modification on Hydrogarnets Formation during Hydrothermal Synthesis. *Cem. Concr.* **2003**, *33*, 1789–1793. [[CrossRef](#)]
34. Mehta, P.K.; Klein, A. Formation of Ettringite in Pastes Containing Calcium Aluminoferrites and Gypsum. 1965, pp. 36–45. Available online: <https://onlinepubs.trb.org/Onlinepubs/hrr/1967/192/192-003.pdf> (accessed on 12 June 2022).
35. Kyritsis, K.; Meller, N.; Hall, C. Chemistry and Morphology of Hydrogarnets Formed in Cement-Based CASH Hydroceramics Cured at 200° to 350 °C. *Am. J. Ceram. Soc.* **2009**, *92*, 1105–1111. [[CrossRef](#)]